JMEPEG (2009) 18:1005–1011
DOI: 10.1007/s11665-008-9340-3

1059-9495/$19.00

Finite Element Method Simulations to Improve Press Formability of Door Hinge

Nguyen Duc Toan, Choi Seogou, Park Junyoung, Suh Yeongsung, and Kim Youngsuk

(Submitted May 12, 2008; in revised form November 6, 2008)

Door hinges are a key product in the automotive industry. The function of automotive door hinge is not only to close, open, and keep the open angle of the door but also to reduce traumas for passengers in the car when it is hit by another car. However, concentrated stress and strain occur at the corner of this product during forming, which can cause a crack if the shape of this area of the blank is not carefully designed. Accordingly, this article proposes a method for improving the press formability of a door hinge by changing the shape of the concerned area of the blank based on finite element method (FEM) simulations using the explicit dynamic code ABAQUS, version 6.5. The resulting optimized solution for robust forming was a corner radius of 7 mm, protrusion length of 18 mm, and protrusion height of 5 mm.

Keywords crack, door hinge, FEM, formability, optimize, sheet metal, Taguchi

1. Introduction

Sheet metal forming is used in relation to automobiles, airplanes, and container ships to reduce the development time and final product cost. Many sheet metal processing parameters contribute to enhancing the formability, such as the material properties, forming conditions, the shapes of the die and punch, and shapes of the blanks. These factors determine the press formability, as regards the thickness variation, and blank failure after the forming. However, the traditional trial and error methods are no longer valid for designing sheet metal forming processes due to the diversity of shapes and growth in the production ratio. Instead, advanced computer hardware and software have been developed, giving computer simulations a more significant role in the real manufacturing process.

Several simple and effective test methods and simulations have already been developed to evaluate the stamping formability of sheet metal. In the Ohio State University (OSU) formability test (Ref 1), a long, rectangular specimen is uniformly stretched under the action of a long, cylindrical punch with the small radius until specimen failure occurs in the plane-strain deformation mode. As regards studies on the process variables, Kim and Park (Ref 2, 3) clarified the effect of the material and process variables on the formability of the sheet material used. In addition, Kim and Park (Ref 4) also used finite element method (FEM) simulations to investigate the effect of material variables and process variables on the performance of a plane strain stretching (PSS) test, and showed that the predictions of the specimen's deformation characteristics and limiting punch height (LPH) values in the FEM simulations agreed with experimental results. More recently, Kim et al. (Ref 5) used FE simulations according to the orthogonal array of Taguchi's method to determine the effect of forming variables on the stamping formability and investigate the effect of design variables on the quality characteristics of the product. They showed that local necking was very sensitive to the plastic-anisotropy parameter of the sheet and friction coefficient at the contact surface. Kim et al. (Ref 6) also showed that optimization of the tool geometry for a plane-strain-punch-stretching test, using an ellipsoidal shape, exhibited a stable performance when evaluating the stamping formability of sheet materials.

When manufacturing a door hinge, as shown in Fig. 1, product failure frequently occurs in the critical area when subjected to the flange bending mode.

In previous literature (Ref 7, 8), this kind of flange failure normally occurs due to metallurgical aspects, such as nonmetallic inclusions, or low ductility of the materials and a high stress level due to inadequate forming conditions, such as poor lubrication and die/design, and a poor surface finish in the shearing/punching process.

Flange failures also start to prevail when increasing the strength of the sheet material to reduce the weight of the white body of car. This type of door hinge failure can be solved by changing the forming conditions, the shape of the die and punch, or modifying the shape of the blank. Accordingly, this study improves the door hinge press formability by decreasing the high stress level based on changing the shape of the blank in the concerned area. As a result, optimizing the blank shape of the door hinge using FE simulation software (ABAQUS version 6.5, explicit formulation) (Ref 9) is shown to be a

Nguyen Duc Toan and **Kim Youngsuk**, Department of Mechanical Engineering, Kyungpook National University, 1370 Sangyeok, Buk-ku, Daegu 702-701, Republic of Korea; **Choi Seogou**, Digital Production Processing and Forming Team, Korea Institute of Industrial Technology, 7-47 Songdo-dong, Songdo-ku, Incheon 406-840, Republic of Korea; **Park Junyoung**, Department of Mechanical Engineering, Kumoh National Institute of Technology, 1 Yangho-dong, Gumi, Gyeongbuk 730-701, Republic of Korea; and **Suh Yeongsung**, Department of Mechanical Engineering, Hannam University, 133 Ojeong-dong, Daedeok-gu, Daejeon 306-791, Republic of Korea. Contact e-mail: caekim@knu.ac.kr.

realistic and cost-effective method that avoids changing the tool.

First, the results from a FE simulation with a cracked test sample are presented (Fig. 2), followed by a comparison with the results from simulations using changed blank-shapes in the concerned area. The relative geometries are then investigated to determine their influence on the press formability. Finally, the optimum geometry is presented according to Taguchi's experimental technique to achieve the optimum shape in the concerned area of the blank (Ref 5, 6, 10-12).

2. Finite Element Simulation

This study used the commercial software ABAQUS version 6.5 to simulate the forming process. This software can provide elastic-plastic and rigid-plastic simulations of metal forming in the case of a large deformation, thereby significantly reducing the cost and time involved in tool and die design.

The flow pattern, equivalent stress distribution, equivalent strain distribution, and major and minor strains can all be simulated by FEM. These simulation results can then be used to obtain the product geometric profile and material properties required. In the preprocess of modeling metal forming, the 3D mechanical type, geometric profile of the blank, and contact surfaces are constructed using the GUI interface of ABAQUS version 6.5.1. An elastic-plastic model is then selected and the material properties, such as Young's modulus, Poisson's ratio, and the density, are needed. The isotropic work-hardening rule is assumed in the flow rule due to plastic strain hardening. The changes in the von Mises stress, major and minor strains yielded on the surface are plotted. The initial conditions of the components are set-up, and the contact between the blank, punch, and die is defined.

Fig. 1 Failure of product in critical area

2.1 Geometry and Models

Figure 3 shows the finite element model of ABAQUS version 6.5 for the forming test process. Here, the punch and die model were made from the shape of the product using CATIA software, the blank modeled using solid elements C3D8R, and the punch and die modeled using rigid surface elements R3D4 with three integration points. Throughout this study, the uniform mesh is used for both solid and rigid surface elements. The average element size of solid elements was about 1 mm in width, 1 mm in length, and 1 mm in height. The average element size of rigid surface elements was about 1.5 mm in width and 1.5 mm in length.

2.2 Material Properties

Table 1 shows the mechanical properties of the blank, a SAPH-440-P sheet steel. The parameters characterizing the uniaxial-stress-plastic-strain response of the material used in the FE simulations are also given in the table in terms of the parameters in Krukowsky's work-hardening law, using the following expression:

$$\sigma = K(\varepsilon_0 + \varepsilon)^n \qquad \text{(Eq 1)}$$

where K is the plastic coefficient, n is the work-hardening exponent, and σ, ε, and ε_0 are the equivalent stress, equivalent strain, and offset strain, respectively.

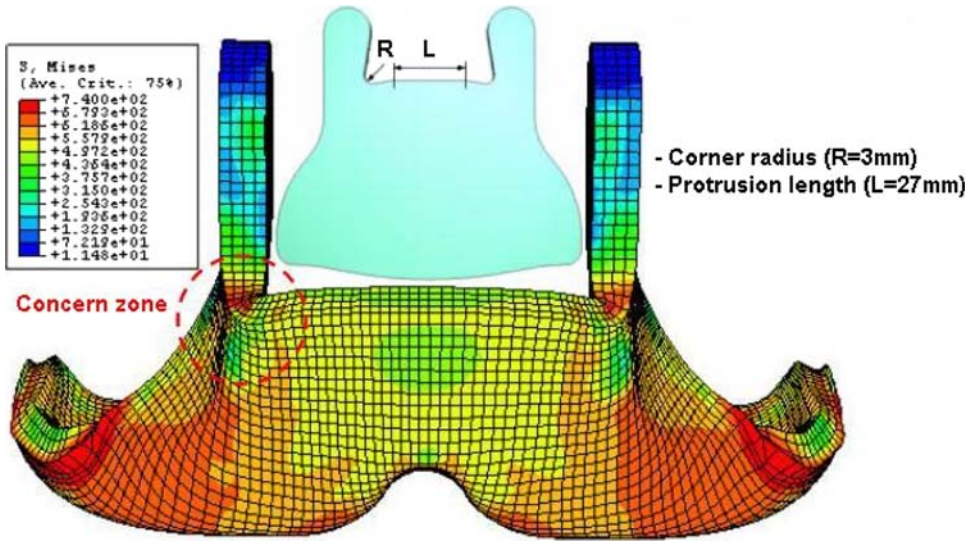

Fig. 2 Deformed shape in finite element simulation of product failure: S, Mises = 714 MPa; $\varepsilon_{max} = 0.8823$; $\varepsilon_{min} = -0.4846$

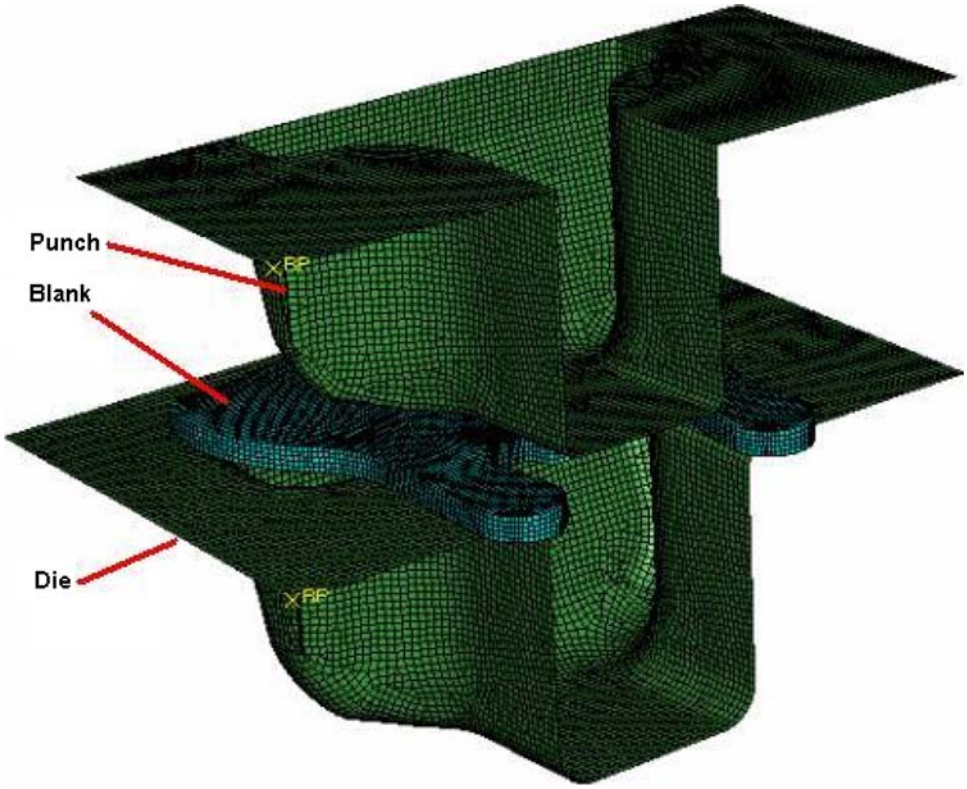

Fig. 3 Finite element model for test simulation

Table 1 Mechanical properties of tested material

Material	SAPH-440-P
Density (ρ), kg/mm^3	7.8e-06
Young's modulus (E), kN/mm^2	210
Thickness (t), mm	5
K, MPa	740
ε_0	0.007
n-Value	0.1604

2.3 Boundary Conditions, Loading, and Interactions

The die was fixed in all directions. The punch was only allowed to move in the vertical direction. The friction behavior was modeled using the Coulomb friction law. The friction coefficients between the blank and the punch/die were $\mu_1 = \mu_2 = 0.1$, as used in previously reported FEM simulations.

3. Taguchi Orthogonal Array

During the forming of a door hinge, a crack will appear if the shape of the concerned area of the blank is not suitably designed. There are two reasons for this: first, the high tensile stress, i.e. the von Mises stress (σ_Y) at the corner of this area, and second the small difference between the major strains (ε_1) and the FLC values at the same point for the minor strains (ε_2) at the corner of this area ($\Delta\varepsilon = \varepsilon_{FLC} - \varepsilon_1$). The forming limit curve (FLC) on right-hand side was determined based on Hecker's punch stretching test (Ref 11). When changing the

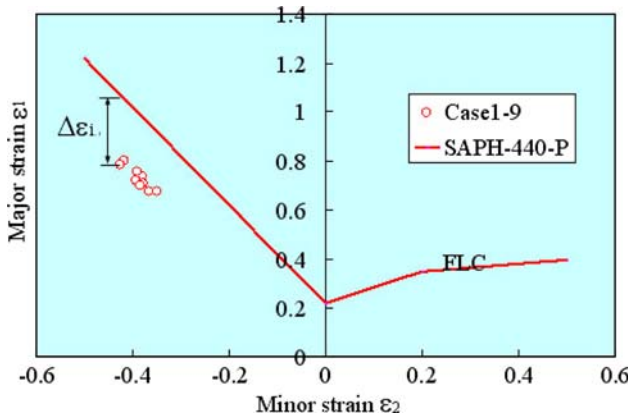

Fig. 4 Forming limit curve and strain distribution for simulation cases

geometry of the concerned area, it was found that the magnitude of the von Mises stress (σ_Y) and difference in the major strain ($\Delta\varepsilon$) also changed. Thus, it was concluded that the geometry of the concerned area of the blank could be optimized. In this study, the FLC's left-side was assumed using the following formulation (see Fig. 4):

$$\varepsilon_1 = -2\varepsilon_2 + 0.22 \quad \text{(Eq 2)}$$

The quality design first proposed by Taguchi in the 1960s is now widely applied due to its proven success in improving industrial product quality (Ref 8-10). Therefore, this study used the Taguchi method to optimize the shape of the concerned area

of the blank. The factors considered here, in order to establish their effect on the forming experiment, were the corner radius (R), protrusion length (L), protrusion height (H), and thickness of the blank (t).

In the preliminary study, the von Mises stress (σ_Y) and difference in the major strain ($\Delta\varepsilon$) were set as the objective functions of the forming experiment, while the three factors—the corner radius (R), protrusion length (L), and protrusion height (H) in the concerned area—were considered as the main changing parameters. An analysis of the selected objective characteristics and values of the von Mises stress (σ_Y) and difference in the major strain ($\Delta\varepsilon$) allowed the level of deviation to be calculated to identify which changing factors were significant for the experiment.

When using this quality characteristic, the problem becomes a smaller-the-better type problem in the case of the von Mises stress (σ_Y) and a larger-the-better type problem in the case of the difference in the major strain ($\Delta\varepsilon$). Thus, according to the Taguchi method, the smaller the von Mises stress (σ_Y) and larger the difference in the major strain ($\Delta\varepsilon$), the better the press formability.

The signal-to-noise ratio (S/N ratio) defined according to the Taguchi method is:

$$\eta_i^a = -10\log_{10}(\sigma_Y^2)$$
$$\eta_i^b = -10\log_{10}(\Delta\varepsilon_1^{-2}) \quad \text{(Eq 3)}$$

where η denotes the observed value (in dB). Since the maximizing procedure for the S/N ratio minimizes the press formability, the best conditions can be obtained by maximizing (η_i).

Figure 5 presents the definition of the three factors, while their selected levels are listed in Table 2.

As the FE simulation using the three factors with three levels gave nine degrees of freedom, a minimum of nine tests were required to investigate the effect on the FE simulation. Table 3 shows the L_9 orthogonal array chosen from Taguchi's standard orthogonal array table. The number for each column is related to the level number for each factor. In this study, only the individual effects of each factor on the FE simulation were investigated, without considering the interactions between each factor.

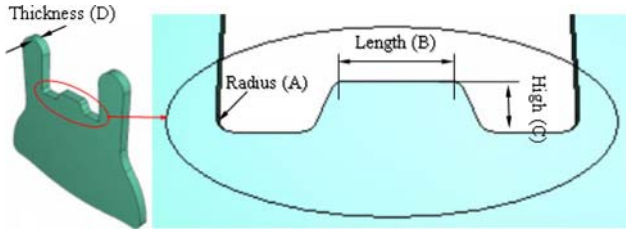

Fig. 5 Definition of factors for concerned area

Table 2 Factors and their levels in FEM simulation

	Level		
Factors, mm	**1**	**2**	**3**
A (R)	3	5	7
B (L)	10	14	18
C (H)	3	5	7
D (t)	5	5	5

4. Results and Discussion

According to the Taguchi method, an analysis of the mean (ANOM) and analysis of variance (ANOVA) were used to represent the relationship between the geometry factors for the concerned area and the observed values for the von Mises stress (σ_Y) and difference in the major strain ($\Delta\varepsilon$). In this experiment, the observed values were found to be related to the three parameters (Table 4). The optimization of the observed values was then determined through a comparison with the Taguchi signal-to-noise (S/N) ratio. The ANOVA values calculated for the three factors and their corresponding three levels (tabulated in Table 2) were obtained using an L_9 orthogonal array. The use of a full factorial design ($3 \times 3 \times 3 \times 3$) reduced the total 81 sets of experiments down to 9, thereby decreasing the cost, time, and effort.

The increase in the factor effect was measured using the S/N ratio of the factors. Moreover, ANOM and ANOVA for the quality characteristics provided a better understanding of the individual effect of each factor. The ANOVA for the different factors—including the level average, total variation, sum of the squares, sum of the mean squares, and contribution—enabled various relative quality effects to be determined.

Tables 5 and 6 show a summary of the calculated results. The formulation used to calculate the sum of the squares was as follows:

$$3(m_{j1} - m)^2 + 3(m_{j2} - m)^2 + 3(m_{j3} - m)^2 \quad \text{(Eq 4)}$$

where m is the overall mean of the η_i, value for the four experiments, defined as $m = 1/9\sum_{i=1}^{9}\eta_i$, here, $m^a = -56.80$ (dB) for the von Mises stress (σ_Y), $m^b = -11.538$ (dB) for the difference in the major strain ($\Delta\varepsilon$), and m_i is the average of η related to level i ($i = 1, 2, 3$) of factor j given by $m_{ji} = 1/3\sum_{i=1}^{3}(\eta_j)_i$.

The results of the ANOM and ANOVA for the von Mises stress (σ_Y) (Table 5 and Fig. 6) revealed that the protrusion height (H), which reached 65.65%, made the major contribution to the overall performance. Meanwhile, the contribution percentages for the corner radius (R) and protrusion length (L) were lower at 27.22 and 7.13%, respectively. The contribution percentage for the protrusion length (L) was the smallest at 7.13%. Thus, it was concluded that the protrusion height (H) factor had the most significant affect on the von Mises stress in

Table 3 Taguchi's L_9 orthogonal array for simulations

Case	A (R), mm	B (L), mm	C (H), mm	D (t), mm
1	1(3)	1(10)	1(3)	1(5)
2	1(3)	2(14)	2(5)	1(5)
3	1(3)	3(18)	3(7)	1(5)
4	2(5)	1(10)	2(5)	1(5)
5	2(5)	2(14)	3(7)	1(5)
6	2(5)	3(18)	1(3)	1(5)
7	3(7)	1(10)	3(7)	1(5)
8	3(7)	2(14)	1(3)	1(5)
9	3(7)	3(18)	2(5)	1(5)

Table 4 L_9 orthogonal array and calculated observed values

	Column number and factor assignment				von Mises stress (σ_Y)		Difference in major strain ($\Delta\varepsilon$)	
Case	A (*R*)	B (*L*)	C (*H*)	D (*t*)	σ_Y	η_i^a, dB	$\Delta\varepsilon$	η_i^b, dB
1	1(3)	1(10)	1(3)	1(5)	711	−57.03	0.2533	−11.925
2	1(3)	2(14)	2(5)	1(5)	678	−56.62	0.2447	−12.225
3	1(3)	3(18)	3(7)	1(5)	693	−56.81	0.2463	−12.171
4	2(5)	1(10)	2(5)	1(5)	681	−56.66	0.2458	−12.187
5	2(5)	2(14)	3(7)	1(5)	718	−57.1	0.2664	−11.487
6	2(5)	3(18)	1(3)	1(5)	710	−57.02	0.2849	−10.905
7	3(7)	1(10)	3(7)	1(5)	694	56.84	0.2726	−11.288
8	3(7)	2(14)	1(3)	1(5)	690	−56.78	0.2862	−10.865
9	3(7)	3(18)	2(5)	1(5)	652	−56.29	0.2888	−10.789

(1) Smaller-the-better type $\eta_i^a = -10\log_{10}(\sigma_Y^2)$
(2) Larger-the-better type $\eta_i^b = -10\log_{10}(\Delta\varepsilon_1^{-2})$

Table 5 ANOM and ANOVA table for affect on von Mises stress (σ_Y)

	Average η by level						
Factor	1	2	3	Sum of squares	DOF	Sum of mean squares	Contribution
A (*R*)	−56.82	−56.93	−56.63 (a)	0.1409	2	0.07045	0.2722
B (*L*)	−56.84	−56.84	−56.70 (a)	0.0369 (b)	2	0.01845	0.0713
C (*H*)	−56.94	−56.52 (a)	−56.92	0.3399	2	0.16995	0.6565
D (*t*)	…	…	…	…	…	…	
Total				0.5177	6	0.25885	

(a) Indicates the optimum level
(b) Indicates the sum of squares added to estimate the pooled error sum of squares in parentheses

Table 6 ANOM and ANOVA table for affect of difference in major strain ($\Delta\varepsilon$)

	Average η by level						
Factor	1	2	3	Sum of squares	DOF	Sum of mean squares	Contribution
A (*R*)	−12.108	−11.526	−10.981 (a)	1.9046	2	0.9523	0.6976
B (*L*)	−11.800	−11.526	−11.288 (a)	0.3930 (b)	2	0.1956	0.1439
C (*H*)	−11.232 (a)	−11.734	−11.649	0.4326 (b)	2	0.2163	0.1585
D (*t*)	…	…	…	…	…	…	
Total				2.7302	6	1.3651	

(a) Indicates the optimum level
(b) Indicates the sum of squares added to estimate the pooled error sum of squares in parentheses

the concerned area, while the effect of the protrusion length (*L*) was negligible.

The η (dB) of the levels for each factor were individually calculated, as shown in Table 4. In the Taguchi method, the higher the η value, the better the overall performance, meaning that the factor levels with the highest η value should always be selected. Accordingly, the average for each experimental level was calculated using the highest η value for each factor to produce the response table (Table 5) and response graph (Fig. 6). As shown in the response table and response graph, the optimum conditions to maintain the von Mises stress (σ_Y) successfully in the forming test were $A_3B_3C_2D_1$, which means R = 7 mm, L = 18 mm, H = 5 mm, and t = 5 mm in Table 3. The *S*/*N* ratio for these optimum conditions is denoted by η_{opt} and predicted as:

$$\eta_{opt} = m + (m_{C2} - m) + (m_{A3} - m) = -56.35\,(\text{dB}) \quad \text{(Eq 5)}$$

An ANOM and ANOVA for the difference in the major strain ($\Delta\varepsilon$) were also carried out, and the results listed in Table 6 and Fig. 7 show the factor effects on the *S*/*N* ratio for the difference in the major strain ($\Delta\varepsilon$). According to the ANOM and Fig. 7, the optimum conditions for the factors were $A_3B_3C_1D_1$, which means R = 7 mm, L = 18 mm, H = 5 mm, and t = 5 mm in Table 3. Meanwhile, according to the ANOVA, the A factor, the corner radius (*R*), which reached

69.76%, made the major contribution to the overall performance, whereas the contribution percentages for the protrusion length (L) and protrusion height (H) were lower at 14.39 and 15.85%, respectively. Thus, it was concluded that the corner radius (R) factor had the most significant effect on the difference in the major strain ($\Delta\varepsilon$) in the concerned area.

The S/N ratio for these selected optimum conditions is denoted by η_{opt} and predicted as:

$$\eta_{opt} = m + (m_{A3} - m) + (m_{C1} - m) = -10.675\,(\text{dB}) \quad \text{(Eq 6)}$$

In this study, the optimum conditions for the press formability were consistent with case no. 9 in Taguchi's orthogonal array.

Figures 8 and 9 show the FE simulation and experimental results for the optimized blank geometry of the concerned area. No crack appeared at the corner of the concerned area.

From the above discussion, it was concluded that the use of Taguchi's experimental array for FE simulations allowed successful optimization of the shape of the concerned area of the blank to improve the press formability. As a result, the shape of the concerned area of the blank was optimized using a corner radius (R) of 7 mm, protrusion length (L) of 18 mm, protrusion height (H) of 5 mm, and blank thickness (t) of 5 mm.

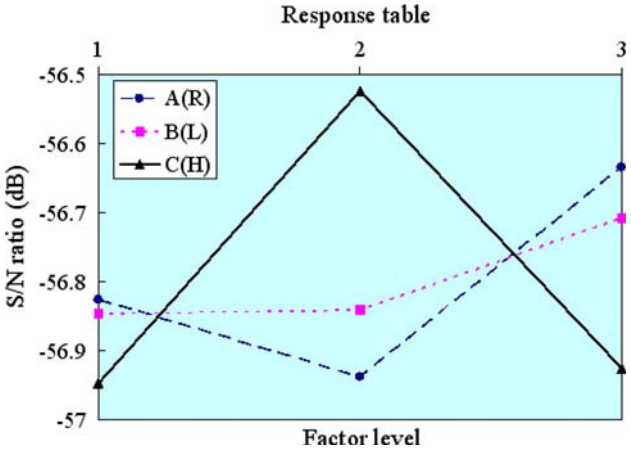

Fig. 6 Factor effects for S/N ratio η_i^a

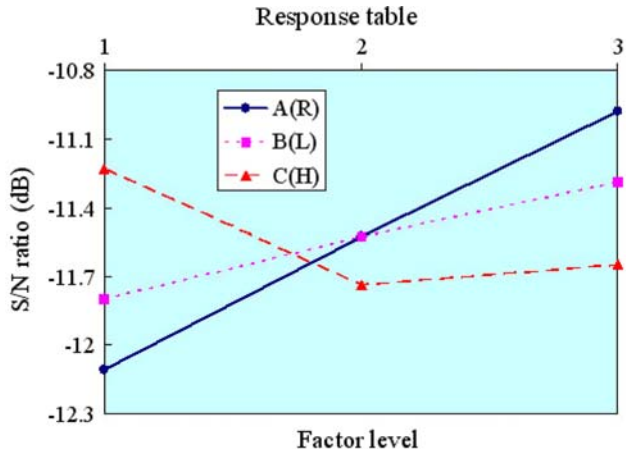

Fig. 7 Factor effects for S/N ratio η_i^b

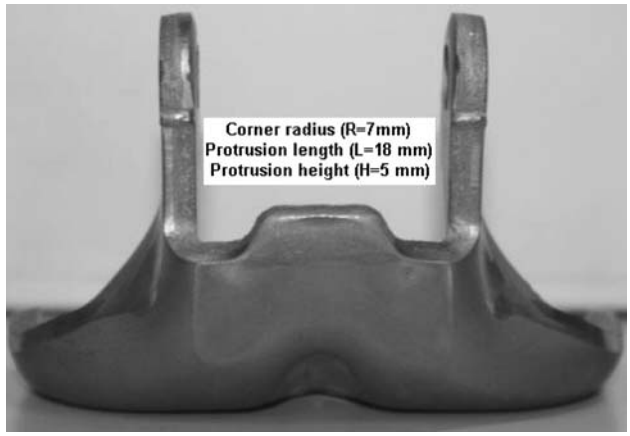

Fig. 9 Optimized product for case no. 9

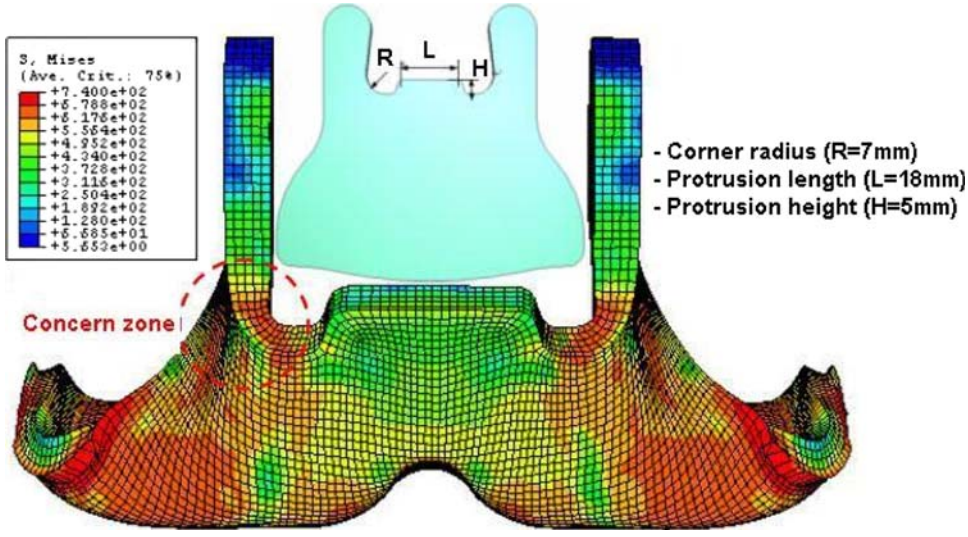

Fig. 8 Deformed shape in finite element simulation of case no. 9: S, Mises = 652 MPa; $\varepsilon_{max} = 0.7010$; $\varepsilon_{min} = -0.3849$

5. Conclusion

To improve the press formability, the shape of the concerned area of a blank was optimized using finite element simulations and then investigated by experiments. Commercial software (ABAQUS version 6.5, explicit formulation) was used for the simulation according to the orthogonal array of Taguchi's method. As a result of the FE simulations based on the Taguchi orthogonal array, the corner radius (R), and protrusion height (H) were identified as the important factors for improving the press formability of the door hinge. An optimized shape for the concerned area of the blank, consisting of a corner radius (R) of 7 mm, protrusion length (L) of 18 mm, a protrusion height (H) of 5 mm, and blank thickness (t) of 5 mm, was also predicted to show a better reliability compared to the original test sample.

This kind approach to optimize the forming process of door hinge using FEM and Taguchi orthogonal experimental method can be used for other forming processes.

The combination with FEM and Taguchi orthogonal experimental method clarity quantitatively clarifies the effect of each main parameter, which assists the optimal design of forming processes.

Acknowledgments

This study was supported from Brain Korea 21 project of Kyungpook National University sponsored from Ministry of Education, Science and Technology is acknowledged.

References

1. F.I. Saunders and R.H. Wagoner, *Computer Application in Shaping & Forming of Materials*, M.Y. Demeri, Ed., TMS, Warrendalem, PA, 1992, p 205–20
2. Y.S. Kim and K.C. Park, Development of Plane Strain Punch Stretching Test, *J. Kor. Soc. Mech. Eng.*, 1993, **7**(5), p 1132–1137
3. Y.S. Kim and K.C. Park, A Plane Strain Punch Stretching Test for Evaluating Stamping Formability of Steel Sheets, *Metall. Mater. Trans. A*, 1994, **25A**, p 2199–2205
4. Y.S. Kim and C.D. Park, A Numerical and Experimental Study of Deformation Characteristics of the Plane Strain Punch Stretching Test, *Metall. Mater. Trans. A*, 1997, **28A**, p 1653–1659
5. Y.S. Kim and K.C. Park, Sensitivity Analysis of Material and Process Variables Affecting on the Stamping Formability, *J. Kor. Soc. Mech. Eng. A*, 1996, **20**, p 2246–2256
6. Y.S. Kim, J.B. Nam, M.S. Chu, and Y.D. Kwon, The Use of the Finite-Element Method to Design an Optimized Tool for the Plain-Strain Punch Stretching Test, *Metall. Mater. Trans. A*, 2000, **31A**, p 93–98
7. D.I. Hyun, S.M. Oak, S.S. Kang, and Y.H. Moon, Estimation of Hole Flangeability for High Strength Steel Plates, *J. Mater. Process. Technol.*, 2002, **130–131**, p 9–13
8. E.E. Cabezas and D.J. Celentano, Experimental and Numerical Analysis of the Tensile Test Using Sheet Specimens, *Finite Elem. Anal. Des.*, 2004, **40**(5–6), p 555–575
9. ABAQUS version 6.5.1, *Analysis User's Manual*, online document
10. G. Taguchi, E.A. Elsayed, and T. Hsiang, *Quality Engineering in Production Systems*, McGraw-Hill, New York, 1989
11. A. Bendell, J. Disney, and W.A. Pridmore, *Taguchi Methods—Application in World Application*, Industries, Productivity, Improvement and Case Study, IFS Publication, UK, 1989
12. G. Taguchi, *On-line Quality Control During Production*, Japan Standard Association, Tokyo, 1981
13. Y.S. Kim, *Theory of Engineering Plasticity*, Sigma Press, Seoul, 2001